Comparison of the effects of PTH (1-34), PTHrP (1-36) and abaloparatide on the murine osteoblast transcriptome.

Michael J Mosca[1,2], Zhiming He[1], Florante R. Ricarte[1], Carole Le Henaff[1], and Nicola C. Partridge[1]

[1] Department of Molecular Pathobiology, New York University College of Dentistry, New York, NY, 10010, USA.

[2] Vilcek Institute of Graduate Biomedical Sciences, New York University School of Medicine, New York, NY, 10016, USA.

Running title: Comparative effects of PTH (1-34), PTHrP (1-36) and abaloparatide on osteoblastic gene expression.

Corresponding Author: Nicola C. Partridge, Ph.D.
Department of Molecular Pathobiology
New York University College of Dentistry
345 East 24th St, Rm 1025B
New York, NY, 10010, USA
ncp234@nyu.edu
1-212-992-7145

Keywords: Osteoblast; Parathyroid hormone (PTH); Osteoporosis; Abaloparatide; RNA-Seq; Transcription

Abstract

Osteoporosis is a prevalent disease with substantial morbidity/mortality among the aging population. Due to gaps in knowledge, current therapeutics are limited in their ability to prevent degeneration of bone while also stimulating formation of new bone. Teriparatide (PTH (1-34)) and its analogs PTHrP (1-36) and abaloparatide (ABL), have been tested and/or utilized for treatment of osteoporosis but have significant limitations in efficacy over long-term use. Research from our laboratory has shown PTH (1-34), PTHrP (1-36), and ABL exert time and dose-dependent differential responses in the osteoblast, leading us to hypothesize they may also differentially modulate the osteoblast transcriptome. In this study we show that treatment of mouse calvarial osteoblasts with 1 nM of these peptides for 4 h results in differing effects on the osteoblast transcriptome by performing gene enrichment analysis of RNA-Seq data. Genes were selected with a Log_2 fold change >1 and a false discovery rate <0.05. These data were analyzed and compiled into heat maps and smear/volcano plots for each peptide. RNA-Sequencing revealed that PTH (1-34) regulated 367 genes, 194 were unique; PTHrP (1-36) regulated 117 genes, 15 were unique; ABL regulated 179 genes, 20 were unique. There were 74 genes shared only among PTH(1-34) and ABL; 16 genes were shared only among PTH (1-34) and PTHrP; and 83 genes were shared among all three peptides. Gene ontology analyses show biological processes are similar between the three peptides but have some pathway-specific differences. Further analysis of the data illuminated that the three peptides increased expression of *Vitamin D receptor* (*Vdr*), *Phosphodiesterase 10a* (*Pde10a*), *Cbp/p300-interacting transactivator 1* (*Cited1*), *Wnt family member 11* (*Wnt11*), and *Secreted frizzled related protein 4* (*Sfrp4)* mRNAs similarly to *Rankl* expression, i.e.,

in a differential expression pattern. These findings were confirmed via qRT-PCR of additional cultured samples of mouse calvarial osteoblasts, treated with 1 nM of PTH (1-34), PTHrP (1-36), or ABL for 4 h prior to harvest. Additionally, we analyzed mRNA abundance of several genes of interest, including *Wnt4*, *Wnt7*, *Dkk1*, *Kcnk10*, *Hdac4*, *Epha3*, *Tcf7*, *Fzd5*, *Pp2r2a*, and *Dvl3* based on genes and pathways chosen from ontology analyses to be significantly regulated by each peptide. Our findings highlight the complexity of the genetic and functional events triggered by PTH (1-34) and its analogs. Many studies have examined PTH signaling in the osteoblast/osteocyte; ours is the first to examine global effects of these three peptides on the osteoblast transcriptome. Further delineation of which signaling events are attributable to PTH (1-34), PTHrP (1-36), and ABL exclusively and which are shared among all three will further our understanding of the effects these peptides have on the osteoblast and lead to refinement of PTH-derived treatments for osteoporosis.

1. Introduction

Osteoporosis, characterized by a decrease in density and quality of bone tissue, is a highly prevalent disease with substantial morbidity/mortality among the aging population. Patients with this pathology have increased risk of fractures that contribute to chronic pain, long-term disability and up to a 20% mortality rate post-operation [1]. Normal physiological processes that maintain healthy bone require the coordination of several complex biochemical pathways that ultimately lead to formation of new bone via osteoblasts and removal of old/damaged bone via osteoclasts [2]. It is critical that these mechanisms remain unperturbed since dysregulation increases the risk of osteoporotic insult through diminished quality and density of bone tissue [3]. The exact mechanisms underpinning proper bone healing are a subject of ongoing research and due to gaps in knowledge our current therapeutics are limited in their ability to prevent degeneration of bone while simultaneously stimulating formation of new bone [4]. Standard treatment with bisphosphonates can mitigate bone resorption, but without stimulating anabolism, osteoporotic tissue cannot form new bone [5].

Parathyroid hormone (PTH), secreted in response to low serum calcium levels, is a key regulator of bone homeostasis, and along with its therapeutic analogs, has been utilized for anabolic treatment of osteoporosis [4,6]. PTH can lead to anabolic effects by decreasing osteoblast apoptosis, by promoting osteoblast differentiation from progenitor cells, by reactivating quiescent bone-lining cells, recruiting stem cells, and stimulating the Wnt pathway by decreasing sclerostin expression by osteocytes [7-11]. PTH can also cause catabolic effects through monocyte chemoattractant protein-1, the receptor

activator of nuclear factor kappa-B ligand (RANKL) / osteoprotegerin (OPG) system, and through protease production [12-15].

Treatment of osteoporosis with PTH and its analogs has positive short-term results due to their osteoanabolic effects, however, with prolonged use, the catabolic effects eventually overshadow the anabolic healing [16]. This phenomenon, defined as the "anabolic window," is the ~0-24 month period during which the positive osteoanabolic effects of PTH-treatment outweigh the deleterious effects of catabolism [4]. RANKL, a pro-osteoclastogenic cytokine with roles in crosstalk between osteoblasts/osteoclasts, is well documented to not only be upregulated by PTH in bone but is also a major source of the catabolic effects affecting the anabolic window, resulting in the limitations of PTH-derived therapeutics [17-19].

Teriparatide (PTH(1-34)), a recombinant form of PTH, was the first osteoanabolic therapeutic to be approved by the United States Food and Drug Administration (FDA). Abaloparatide (ABL), an analog of parathyroid hormone-related protein (PTHrP(1-34)), became the second FDA-approved osteoanabolic for treatment of osteoporosis and has been shown to be somewhat more effective in producing osteoanabolic outcomes compared with teriparatide; ABL resulted in higher bone mineral density (BMD) in the femurs of osteoporotic, post-menopausal women compared with teriparatide [20-23]. It has also been shown that serum CTX levels, a marker for bone resorption, were lower in patients treated with ABL compared with teriparatide, suggesting it has a lesser tendency to promote deleterious effects [23]. Despite this, neither ABL nor teriparatide have been able to overcome the anabolic window preventing the long-term efficacy of these treatments for osteoporotic patients [24].

PTH, PTHrP, and ABL all bind the same G protein-coupled receptor, parathyroid hormone receptor type 1 (PTHR1) [25]. One study found that PTH (1-34), PTHrP (1-36), and ABL act through two PTHR1 conformations named R^O and R^G. Binding to R^O results in prolonged signaling, which is thought to lead to comparatively more bone resorption, while binding to R^G is thought to result in more osteoanabolic signaling [26]. The study determined that ABL binds with greater selectivity to R^G and concluded this represents a plausible explanation for the favorable anabolic effects of ABL treatment reported on bone compared with PTH (1-34). The differences observed in this study of PTH (1-34), PTHrP (1-36), and ABL binding to PTHR1 suggest that these findings may be reflected by differential signaling events downstream of PTHR1. There is a paucity of data that seeks to determine differences in signaling from PTH (1-34), PTHrP (1-36), and ABL in osteoblast lineages.

There are a variety of signaling cascades that are stimulated upon PTHR1 ligand binding, including 1) GαS–adenylyl cyclase–cAMP–protein kinase A (GαS/cAMP/PKA), 2) Gαq–phospholipase C (PLC) β–inositol triphosphate–cytoplasmic Ca2+–protein kinase C pathway, 3) Gα12/13–phospholipase signaling, 4) and the β-arrestin–extracellular signal-regulated kinase 1/2 (ERK1/2) pathway [27]. The GαS/cAMP/PKA pathway accounts for most of PTHR1 signaling and this is purported to mediate the anabolic response to PTH as well as the catabolic response [17, 28-35]. Recent work from our laboratory examined if PTH (1-34), PTHrP (1-36), and ABL treatment would result in unique stimulatory effects with respect to cAMP production and known downstream effectors of this pathway [36]. We found that in primary murine calvarial osteoblasts, PTHrP (1-36) and ABL result in a significantly lower cAMP response

compared with PTH (1-34). Downstream of this signaling cascade, time course and dose response analyses showed similar relative differences in the phosphorylation of cAMP response element binding protein (CREB), and extracellular signal-regulated protein kinases 1 and 2 (ERK1/2). However, quantitative real-time PCR (qRT-PCR) of known osteoblastic genes found several genes were similarly regulated such as the Wnt inhibitor, *Sost*, while *c-Fos* and *Rankl* were differentially regulated in time and dose-dependent manners.

Since we determined that these peptides differentially exert time and dose-dependent responses in the osteoblast, particularly on the cAMP/PKA/*Fos* or *Rankl* axes, we hypothesized that these changes reflect the ability of PTH (1-34), PTHrP (1-36), and ABL to differentially modulate the osteoblast transcriptome. Several studies have examined PTH signaling in the osteoblast/osteocyte but none to date have examined the global effects of these peptides on the osteoblast transcriptome. In this study, RNA-Sequencing was performed on primary calvarial murine osteoblasts treated with PTH (1-34), PTHrP (1-36), and ABL by repeating the conditions under which we observed differences in *Rankl* expression to examine their global effects on the osteoblast transcriptome [36]. We hypothesized that the differences among these peptides published previously on their binding affinities, clinical outcomes, and downstream expression of anabolic/catabolic effectors would be reflected at the transcriptional level and that unique differences in signaling cascades would be elicited by each peptide, allowing us to determine new signaling biases of interest. If these peptides lead to differential expression of osteoblastic or unknown cascades/genes then it may provide key insights for future

studies to better understand the osteoanabolic and catabolic effects of PTH-derived treatments so that more effective therapeutics can be developed to treat osteoporosis.

2. Materials and Methods

2.1: Peptides and Chemicals

Rat parathyroid hormone (PTH 1-34) was purchased from Bachem. Parathyroid hormone-related protein (PTHrP 1-36) and abaloparatide (ABL) were synthesized by the Peptide/Protein Core Facility at the Massachusetts General Hospital (MGH). All PTH (1-34), PTHrP (1-36), and ABL peptide sequences were confirmed and analyzed for purity and degradation by NYU Grossman School of Medicine Mass Spectrometry Core Facility. All peptides were dissolved in acetic acid at 10 mM. Ascorbic acid was purchased from Sigma. Collagenase A was purchased from Worthington Biochemical Corporation.

2.2: Cell Culture

Primary mouse calvarial osteoblasts were harvested from C57Bl/6J wild-type mice aged 2-3 days postnatal. Mice were euthanized with ketamine (0.25 mg/pup) and xylazine (0.025 mg/pup). Calvariae were digested in 1 mg/mL collagenase A at 37°C by five sequential digestions, and cells from digests 3-5 were collected and plated at a density of 6.4 x 10^3 cells/cm^2 in αMEM supplemented with 10% FBS and 100 units/mL penicillin and 100 ug/mL streptomycin. After reaching confluence, osteogenic medium (50 ug/mL ascorbic acid) was added for 5 days to allow osteoblastic differentiation. Prior to harvest, osteoblasts were treated with 1 nM of the peptides for 4 h (n=3-4 per treatment group). Prior to treatment, cells were serum-starved with 0.1% FBS for 16 h. The osteoblastic phenotype of all primary cells was confirmed by measuring the relative mRNA levels of osteoblastic genes, type-1 collagen and alkaline phosphatase.

2.3: RNA-Sequencing

Total RNA was isolated from cells by using TRIzol reagent (Thermo Scientific, Pittsburgh, PA) and purified with RNeasy mini kit from Qiagen (Valencia, CA). Prior to RNA-seq, the RNA integrity was assessed with Agilent 2100 Bioanalyzer (Santa Clara, CA) and the best quality triplicate samples were chosen for the subsequent analyses. The RNA-seq libraries were constructed using the Illumina TruSeq Stranded Total RNA library prep kit with Ribozero Gold (San Diego, CA). Sequencing was carried out with an Illumina HiSeq 2500 system with paired-end 100 bp reads at the Genome Technology Center of NYU Grossman School of Medicine. The quality of raw data was checked by FastQC (v. 0.11.9), and the read counts were quantified using Salmon (v. 1.7.0) against the GRCm38/mm10 mouse transcriptome reference (UCSC) database [37]. Pairwise differential expression analysis was performed by DESeq2 R/Bioconductor package (v. 1.34.0) [38]. Where gene expression was found to be significantly above ±1.0 log2FC after treatments, these genes were imputed in DAVID Bioinformatics Database NIAID/NIH for Gene Ontology (GO) analyses [39].

2.4: qRT-PCR

Total RNA was extracted using Trizol (Sigma). Complementary DNA (cDNA) was synthesized from 1 ug of total RNA using TaqMan reverse transcription kit (Applied Biosystems) with hexamer primers following the protocol described by the manufacturer. Gene expression levels were measured using SYBR Green polymerase chain reaction Reagents (Applied Biosystems). Primer pairs used for quantitative detection of gene expression are listed in *Appendix A*. The quantity of messenger RNA (mRNA) was

calculated by normalizing the threshold cycle value (Ct) of specific genes to the Ct of the housekeeping genes *β-actin* and/or *Ribosomal protein L13a* (*Rpl13a*).

2.5: Statistics

Statistical differences were analyzed either by Student's t-test or one-way ANOVA using IBM SPSS (v24). Tukey's tests were then performed to determine which groups in the sample differed significantly from one another. Results are expressed as mean ± S.D. and a $p<0.05$ was considered significant comparing treatment groups.

3. Results

3.1 Global Expression Profiles for PTH (1-34), PTHrP (1-36), and ABL

Genes were selected if they had a Log_2 fold change (FC) > 1 and had a false discovery rate (FDR) < 0.05. RNA-Sequencing revealed that PTH (1-34) regulated 367 genes, 194 were unique; PTHrP (1-36) regulated 116 genes, 15 were unique; ABL regulated 179 genes, 20 were unique. There were 74 genes shared only among PTH(1-34) and ABL; 16 genes shared only among PTH (1-34) and PTHrP; and 83 genes shared among all three peptides. These data were analyzed and compiled into Venn diagrams (Fig.1), heat maps comparing peptides (Fig. 2), and volcano plots (Fig. 3). The heat maps show that there is a complete change in gene expression with PTH (1-34) and that this peptide causes greater effects than the other peptides, with PTHrP causing the least effects. The volcano plots further illustrate this and show some of the specific genes regulated.

3.2 Pathway Analyses of PTH (1-34), PTHrP (1-36), and ABL Treatment on the Osteoblast Transcriptome

Analyses of RNA-Seq data were performed using gene ontology to determine pathway-specific trends from differentially expressed genes according to each peptide treatment (Fig. 4). These were analyzed via R to identify the gene ontology biological processes. In this figure the size of the bubbles corresponds to the number of genes each peptide regulated per category and the color represents the level of significance. PTH (1-34) and ABL have similarly high levels of significance for all categories except for “morphogenesis of branching structures”, where ABL does not significantly regulate this

pathway, while PTHrP (1-36) and PTH (1-34) showed more common regulation of genes of this pathway. PTH (1-34) and ABL show an almost identical pattern otherwise, and PTHrP (1-36) regulates these pathways differently when compared with either of these peptides. Some pathways were regulated by all three, some by just two. Notably, PTH (1-34) and ABL similarly regulated genes of “bone mineralization”, “biomineral tissue development” and “actin filament bundle organization”, while PTHrP (1-36) did not regulate these pathways significantly.

Figure 1: Venn Diagram of PTH (1-34), PTHrP (1-36), and ABL Treatment on the Osteoblast Transcriptome. Gene lists were selected with Log_2 Fold Change ≥ 1; False Discovery Rate < 0.05 compared with the vehicle controls. PTH (1-34) regulated 367 genes, 194 were unique; PTHrP (1-36) regulated 116 genes, 15 were unique; ABL regulated 179 genes, 20 were unique. There were 74 genes shared only among PTH(1-34) and ABL; 16 genes shared only among PTH (1-34) and PTHrP; and 83 genes shared among all three peptides.

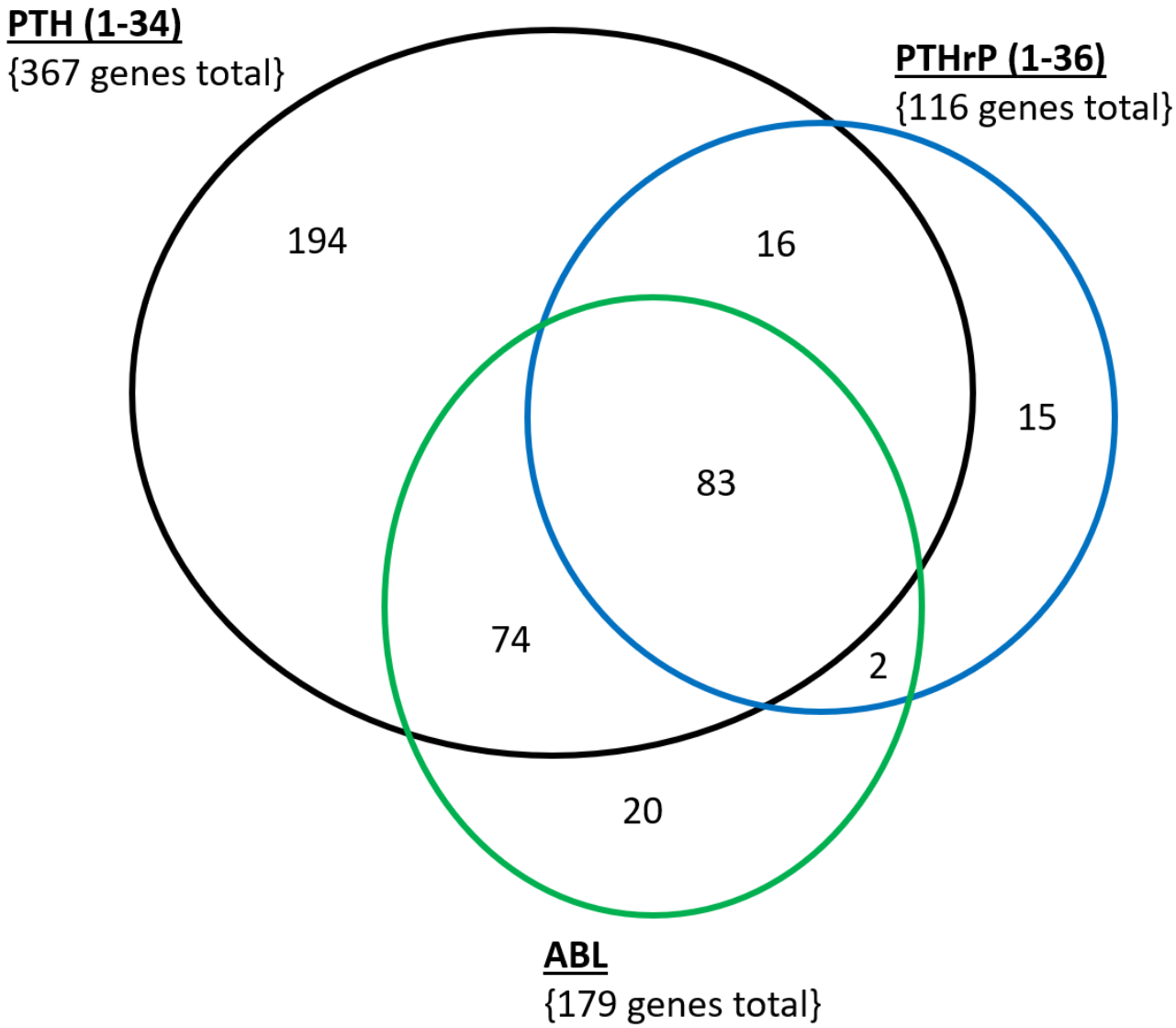

Figure 2: Heat Map of PTH (1-34), PTHrP (1-36), and ABL-regulation of the Osteoblast Transcriptome. Red represents transcript upregulation; blue represents transcript downregulation. Analysis is relative to control samples. Genes were selected if they had a Log_2 fold change (FC) > 1 and had a false discovery rate (FDR) < 0.05.

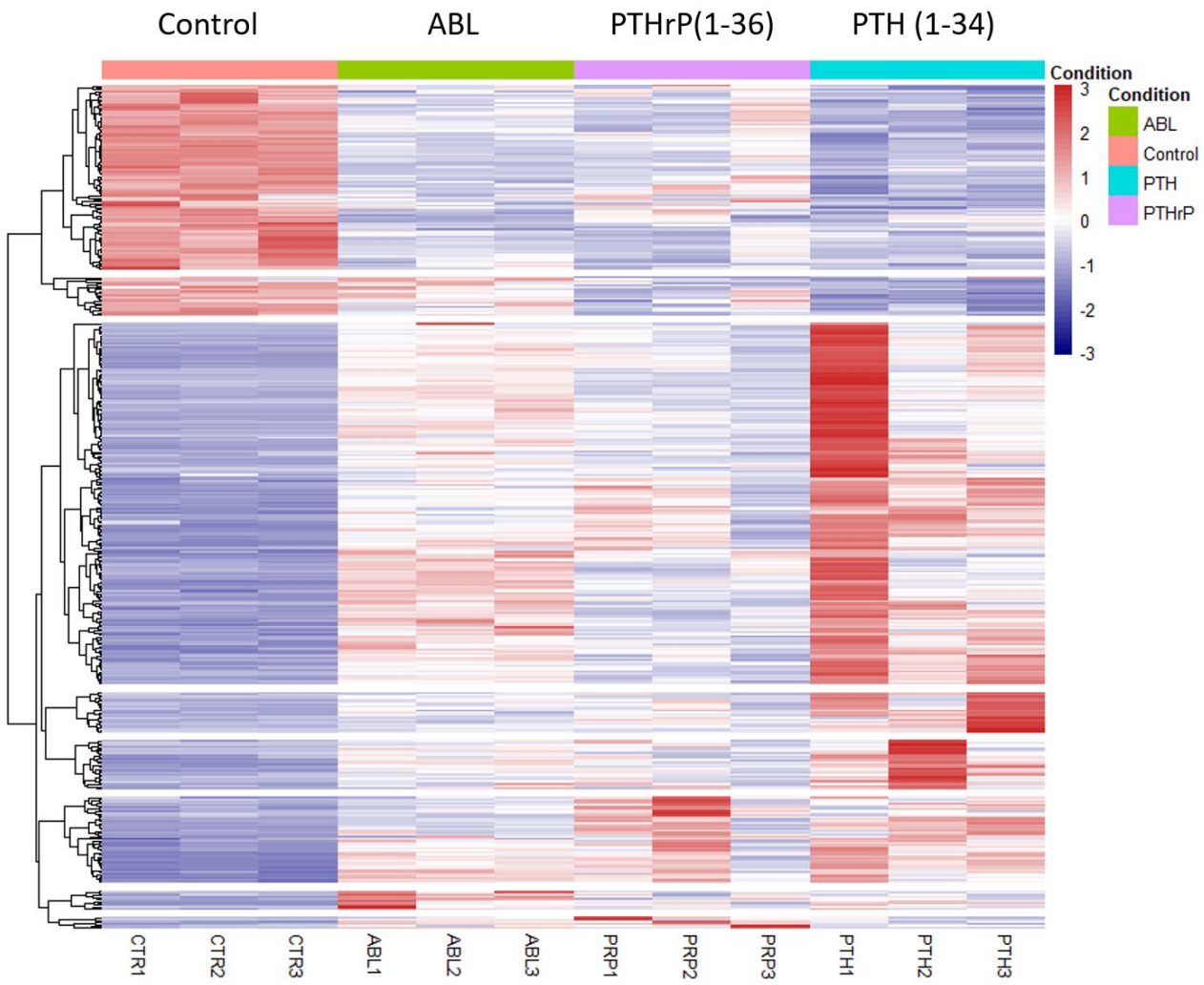

Figure 3: Volcano Plots of PTH (1-34), PTHrP (1-36), and ABL-regulation of the Osteoblast Transcriptome. Genes were selected if they had a Log_2 fold change (FC) > 1 and had a false discovery rate (FDR) < 0.05. (A) Shows PTH (1-34) vs. Control, (B) ABL vs. Control, (C) PTHrP (1-36) vs. Control. Genes which are red on the graph are significantly regulated and have a Log_2 fold change (FC) > 1; genes represented by blue were significantly regulated but did not pass the FC threshold, and genes represented by grey had no significant changes compared to control with either selection.

A)

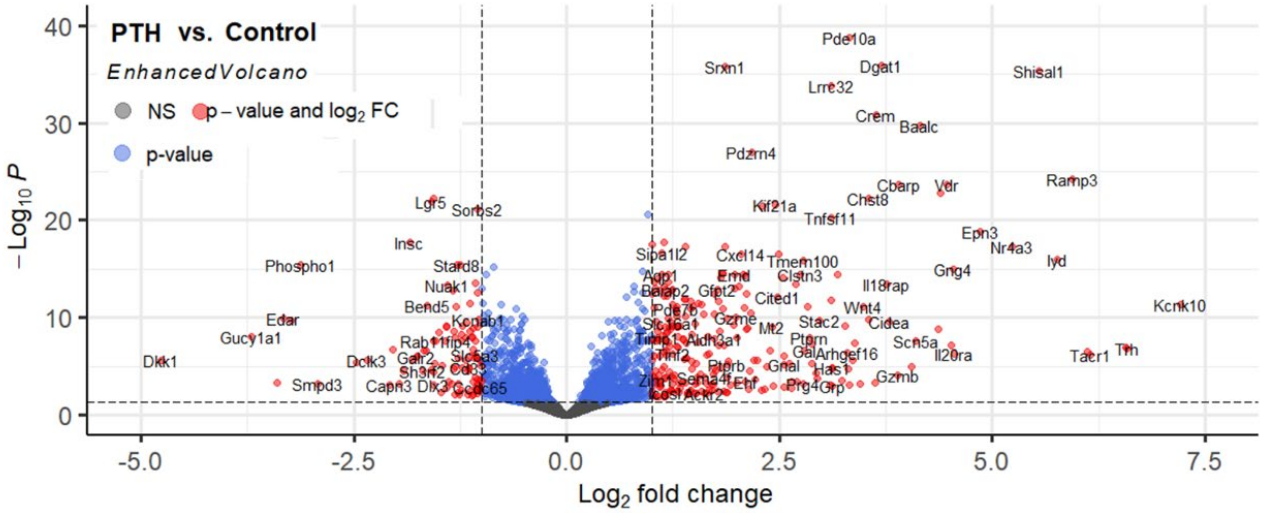

B)

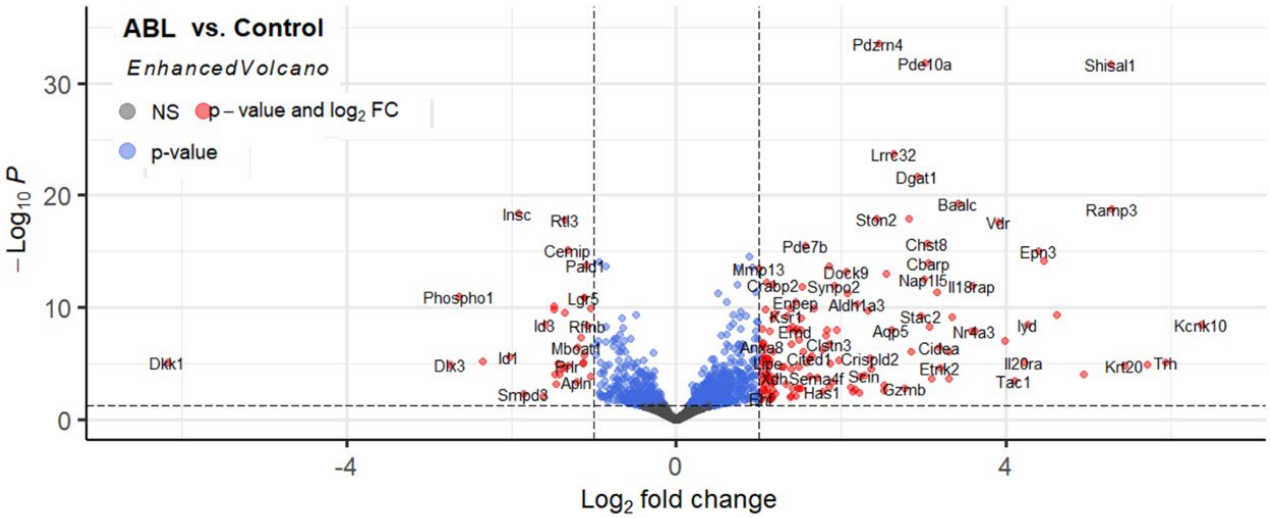
ABL vs. Control
EnhancedVolcano
NS
p – value and log2 FC
p-value
– Log10 P
Log2 fold change
Pdzrn4
Pde10a
Shisal1
Lrrc32
Dgat1
Baalc
Ramp3
Insc
Rtl3
Ston2
Vdr
Cemip
Pde7b
Chst8
Epn3
Pald1
Mmp13
Dock9
Cbarp
Crabp2
Sympo2
Nap1l5
Il18rap
Phospho1
Lgr5
Enpep
Aldh1a3
Ksr1
Stac2
Id3
Rfinb
Emd
Aqp5
Nr4a3
Iyd
Kcnk10
Mboat1
Anxa8
Clstn3
Cidea
Dkk1
Dlx3
Id1
Prlr
Cited1
Crispld2
Il20ra
Krt20
Trh
Apln
Xdh
Sema4f
Scin
Etnk2
Tac1
Smpd3
Has1
Gzmb
Frt

C)

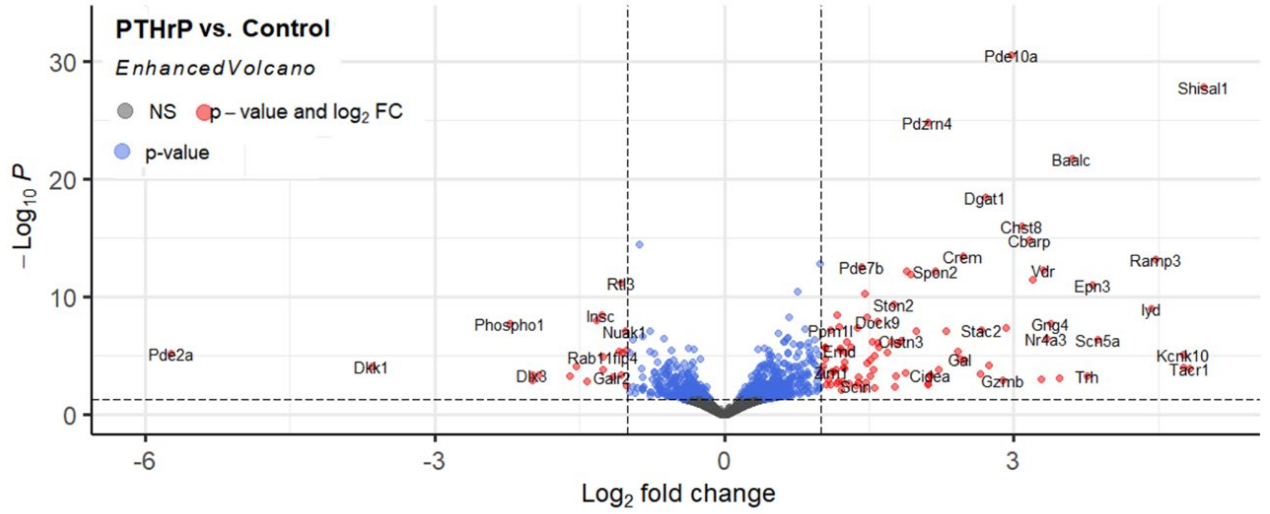
PTHrP vs. Control
EnhancedVolcano
NS
p – value and log2 FC
p-value
– Log10 P
Log2 fold change
Pde10a
Shisal1
Pdzrn4
Baalc
Dgat1
Chst8
Cbarp
Crem
Ramp3
Pde7b
Spon2
Vdr
Epn3
Rtl3
Ston2
Iyd
Insc
Phospho1
Nuak1
Dock9
Ppm1l
Stac2
Gng4
Nr4a3
Scn5a
Clstn3
Pde2a
Rab11fip4
Emd
Gal
Kcnk10
Tacr1
Dkk1
Dlx3
Galr2
Zim1
Cidea
Gzmb
Trh
Scin

Figure 4: Pathway Specific Comparison of PTH (1-34), ABL, and PTHrP (1-36) Treatment on Osteoblast Transcriptome Pathways. If gene expression was found to be above ±1.0 $\log_2$FC genes were imputed in DAVID Bioinformatics Database NIAID/NIH for Gene Ontology (GO) analysis; data for Control vs. peptide were graphed via R.

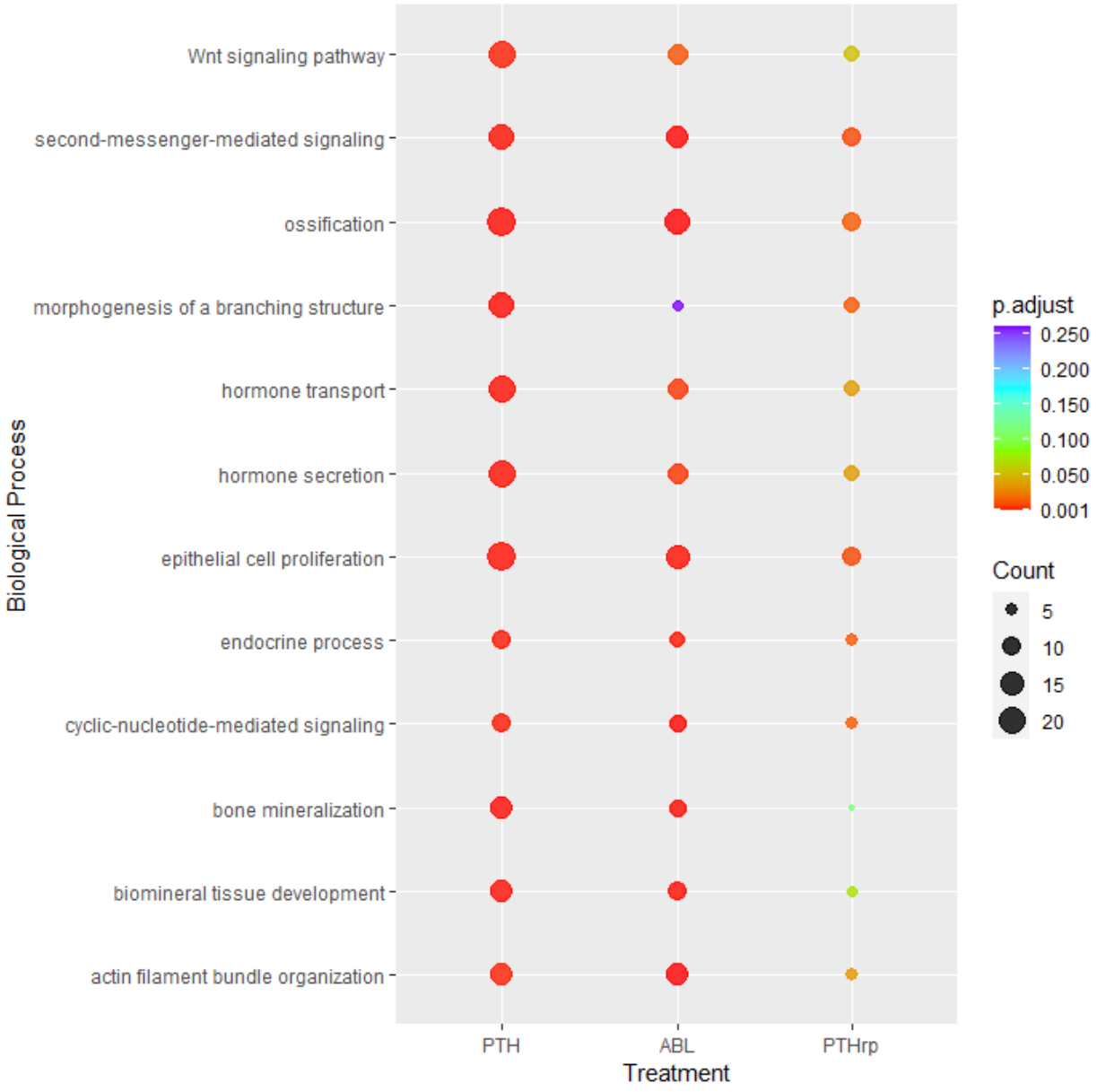

3.3 Examination of genes of interest with RNA-seq data and qRT-PCR verification

Based on these data we selected a number of genes which were highly up or down-regulated to examine more closely and to verify the RNA-seq data with qRT-PCR in separate calvarial osteoblast preparations. The genes included 1) *Cbp/P300 interacting transactivator with Glu/Asp rich carboxy-terminal domain 1* (*Cited1*), 2) *Vitamin D receptor* (*Vdr*), 3) *Phosphodiesterase 10A* (*Pde10a*), 4) *Wnt Family Member 11* (*Wnt11*), 5) *Secreted frizzled related protein 4* (*Sfrp4*), 6) *cAMP responsive element modulator* (*Crem*), 7) *Ephrin type-A receptor 3* (*Epha3*), 8) *Histone deacetylase 4 (Hdac4*), 9) *Protein phosphatase 2 regulatory subunit B alpha* (*Pp2r2a*), 10) *Dishevelled segment polarity protein 3* (*Dvl3*), 11) *Frizzled class receptor 5* (*Fzd5*), 12) *Transcription factor 7* (*T-Cell specific, HMG-box*) (*Tcf7*), and 13) *Potassium two pore domain channel subfamily K member 10* (*Kcnk10*). RNA-seq Log_2 fold changes/p-values are shown in Table 1.

qRT-PCR data confirmed *Vdr*, *Cited1*, *Pde10a*, and *Wnt11* mRNAs followed the reported pattern of expression profiling of *Rankl* in response to these peptides: PTHrP (1-36) and ABL elicit a moderate increase in *Rankl* compared with control with PTHrP (1-36) being in most cases significantly lower than ABL and PTH (1-34) eliciting the greatest increase in expression of these genes compared with control (Fig 5). *Sfrp4* closely mimicked this expression pattern but with one minor difference in just the qPCR data: PTHrP (1-36) resulted in higher mRNA expression than ABL but both were still lower than just PTH (1-34) treatment.

qRT-PCR data showed that *Crem*, *Epha3*, *Hdac4, Pp2r2a, and Dvl3* mRNAs were similarly regulated by all three peptides even if not all were significantly so (Fig 6), confirming the RNA-seq data (Table 1).

Further qPCR analyses show additional mRNA response patterns that mimic their respective RNA-seq data bar one, Kcnk10 (Table 1, yellow star). Wnt4 and Wnt7b are both upregulated by all three peptides compared to control and it is very noticeable that PTHrP yields a significantly greater stimulation of *Wnt4* than the other peptides. *Dkk1*, *Fzd5*, and *Tcf7* are all downregulated by all three peptides (Fig 7). These qPCR data analyses show all three peptides downregulated *Kcnk10* which differs from the RNA seq data which shows upregulation for all three peptides, PTH having the greatest impact of them all.

Table 1: Regulation of genes of interest by RNAseq after PTH (1-34), ABL, and PTHrP (1-36) treatment in differentiating calvarial osteoblasts. (+) log2 FC represents upregulation compared to control; (-) log2 FC represents downregulation compared to control.

Gene ID	Gene Name	PTH (1-34)		ABL		PTHrP (1-36)	
		Log2 FC	p-value	Log2 FC	p-value	Log2 FC	p-value
Cited1	Cbp/P300 Interacting Transactivator 1	2.48	3.56E-15	1.61	3.22E-08	1.56	7.13E-08
Vdr	Vitamin d receptor	4.47	2.31E-24	3.90	1.83E-21	3.31	4.77E-16
Pde10a	Phosphodiesterase 10A	3.34	1.02E-43	3.02	2.21E-36	2.96	2.10E-35
Wnt11	Wnt family member 11	1.52	1.43E-07	1.15	1.27E-05	0.13	ns
Sfrp4	Secreted Frizzled Related Protein 4	1.141	3.00E-07	1.054	3.77E-06	0.355	4.09E-02
Crem	cAMP responsive element modulator	2.30	0.0001	2.82	8.53E-22	2.47	2.21E-17
Epha3	ephrin type-A receptor 3	4.86	3.11E-06	4.35	5.14E-11	4.71	4.65E-05
Hdac4	Histone deacetylase 4	1.33	4.56E-14	1.20	1.33E-12	1.16	5.44E-12
Pp2r2a	Protein Phosphatase 2 Regulatory Subunit B alpha	0.205	2.88E-01	0.013	9.43E-01	0.393	5.23E-02
Dvl3	Dishevelled Segment Polarity Protein 3	0.092	6.42E-01	0.035	8.17E-01	0.756	1.14E-02
Wnt4	Wnt family member 4	3.49	4.68E-14	3.08	2.67E-11	1.18	3.17E-06
Wnt7b	Wnt family member 7b	0.274	1.73E-01	0.397	6.22E-02	0.106	4.09E-01
Dkk1	Dickkopf WNT signaling pathway inhibitor 1	-4.77	2.42E-11	-6.17	7.83E-08	-3.65	8.04E-07
Fzd5	Frizzled Class Receptor 5	-1.279	1.32E-06	-0.805	1.83E-03	-0.154	2.90E-01
Tcf7	Transcription Factor 7 (T-Cell Specific, HMG-Box)	-0.572	3.42E-02	-0.128	3.44E-01	-0.208	1.53E-01
Kcnk 10	Potassium two pore domain channel subfamily K member 10	7.21	4.30E-12	2.83	8.53E-22	4.76	5.49E-08

Figure 5: PTH (1-34), PTHrP (1-36), and ABL Modulate Expression of *Vdr*, *Cited1*, *Pde10a*, *Wnt11, and Sfrp4* mRNA with a Similar Pattern to *Rankl*. Primary differentiating calvarial osteoblasts were treated with 1 nM of PTH (1-34), PTHrP (1-36), or ABL for 4 h prior to harvest, followed by qRT-PCR for *Vdr*, *Cited1*, *Pde10a*, *Wnt11, Sfrp4* and *Rankl* mRNAs. All data are expressed relative to the housekeeping gene *Rpl13a* and represent mean ± S.D. of n=3 independent experiments. * $p < 0.05$, ** $p < 0.01$, *** $p < 0.001$, ns, not significantly different.

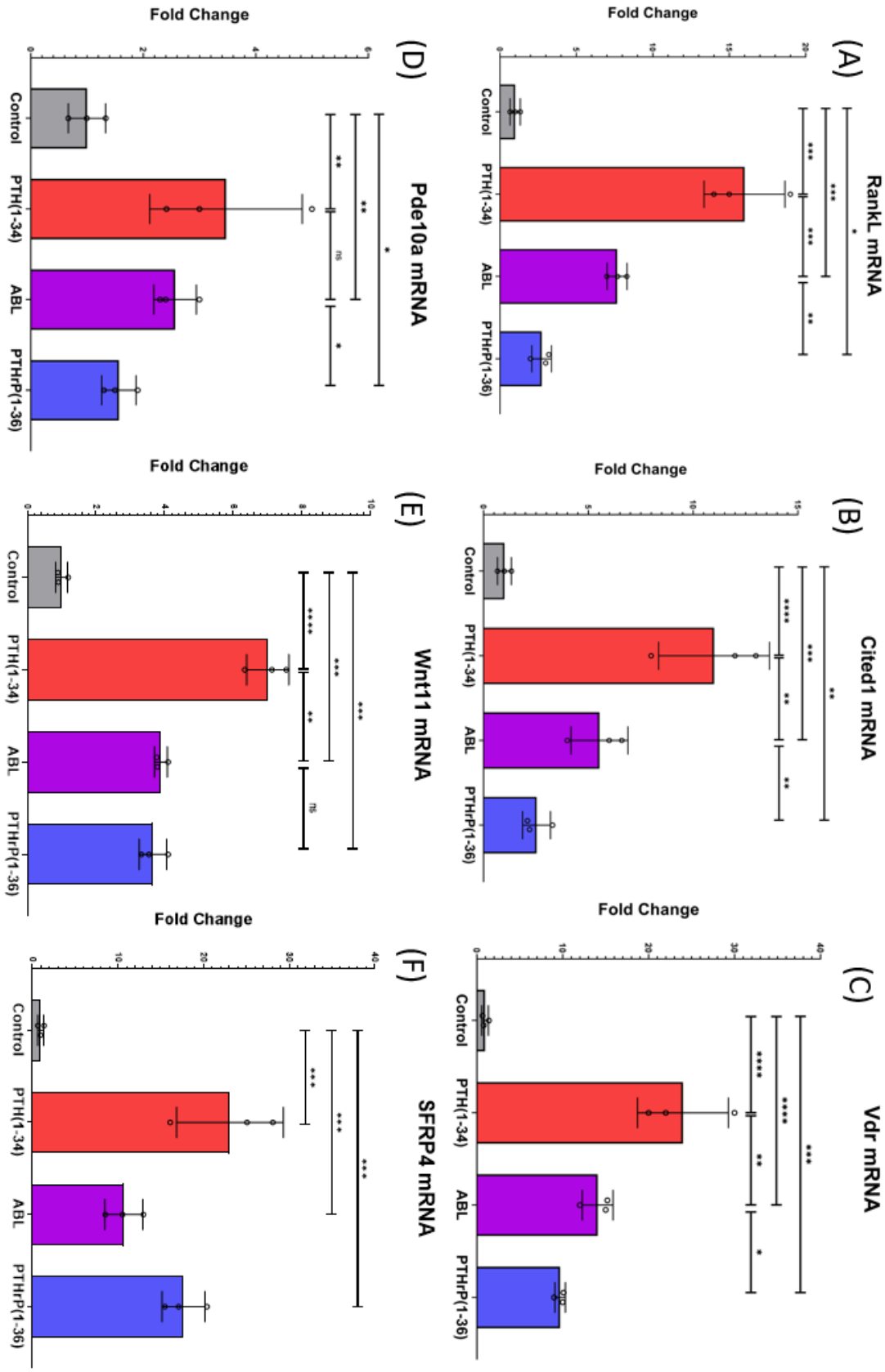
(A)
RankL mRNA
Fold Change
Control
PTH(1-34)
ABL
PTHrP(1-36)
(B)
Cited1 mRNA
Fold Change
Control
PTH(1-34)
ABL
PTHrP(1-36)
(C)
Vdr mRNA
Fold Change
Control
PTH(1-34)
ABL
PTHrP(1-36)
(D)
Pde10a mRNA
Fold Change
Control
PTH(1-34)
ABL
PTHrP(1-36)
(E)
Wnt11 mRNA
Fold Change
Control
PTH(1-34)
ABL
PTHrP(1-36)
(F)
SFRP4 mRNA
Fold Change
Control
PTH(1-34)
ABL
PTHrP(1-36)

Figure 6: PTH (1-34), PTHrP (1-36), and ABL have the Same Effect on *Crem*, *Epha3*, *Hdac4, Pp2r2a, and Dvl3* mRNA Expression. Primary differentiating calvarial osteoblasts were treated with 1 nM of PTH (1-34), PTHrP (1-36), and ABL for 4 h prior to harvest, followed by qRT-PCR for *Crem*, *Epha3*, *Hdac4, Pp2r2a, and Dvl3* mRNAs. All data are expressed relative to the housekeeping gene *β-actin* and represent mean ± S.D. of n=3 independent experiments. * $p < 0.05$, ** $p < 0.01$, *** $p < 0.001$, ns, not significantly different.

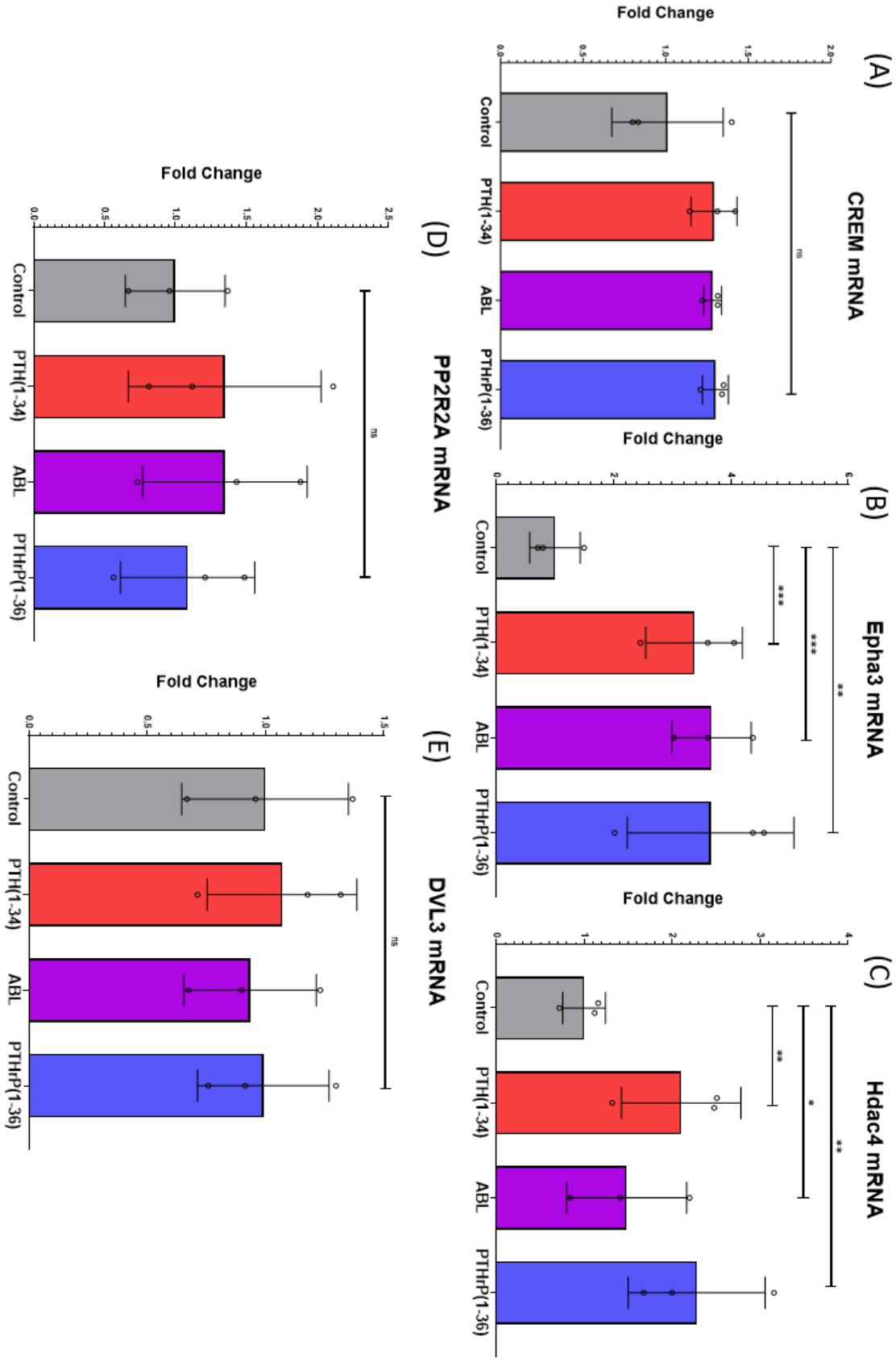
(A)
CREM mRNA
Fold Change
ns
Control
PTH(1-34)
ABL
PTHrP(1-36)
(B)
Epha3 mRNA
Fold Change
**
***
***
Control
PTH(1-34)
ABL
PTHrP(1-36)
(C)
Hdac4 mRNA
Fold Change
**
*
**
Control
PTH(1-34)
ABL
PTHrP(1-36)
(D)
PP2R2A mRNA
Fold Change
ns
Control
PTH(1-34)
ABL
PTHrP(1-36)
(E)
DVL3 mRNA
Fold Change
ns
Control
PTH(1-34)
ABL
PTHrP(1-36)

Figure 7: PTH (1-34), PTHrP (1-36), and ABL Regulation of *Wnt4, Wnt7b, Dkk1*, Fzd5, *Tcf7*, and *Kcnk10* mRNAs. Primary differentiating calvarial osteoblasts were treated with 1 nM peptides for 4 h, followed by qRT-PCR for *Wnt4, Wnt7b, Dkk1, Fzd5, Tcf7, and Kcnk10*. All data are expressed relative to the housekeeping gene *Rpl13a* and represent the mean ± S.D. of n=3 independent experiments. * $p < 0.05$, ** $p < 0.01$, *** $p < 0.001$, ns, not significantly different.

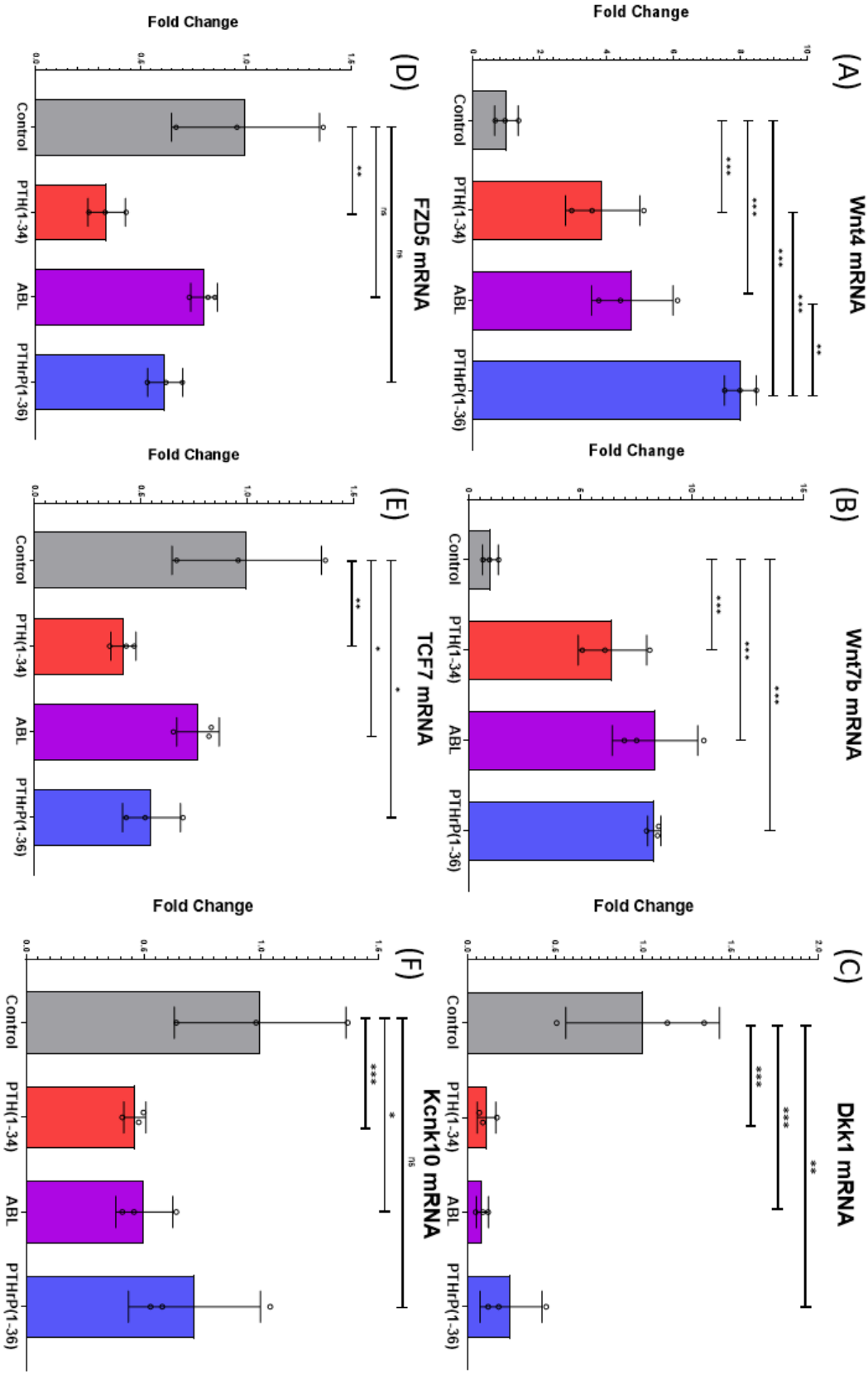
(A)
Wnt4 mRNA
Fold Change
Control
PTH(1-34)
ABL
PTHrP(1-36)
(B)
Wnt7b mRNA
Fold Change
Control
PTH(1-34)
ABL
PTHrP(1-36)
(C)
Dkk1 mRNA
Fold Change
Control
PTH(1-34)
ABL
PTHrP(1-36)
(D)
FZD5 mRNA
Fold Change
Control
PTH(1-34)
ABL
PTHrP(1-36)
(E)
TCF7 mRNA
Fold Change
Control
PTH(1-34)
ABL
PTHrP(1-36)
(F)
Kcnk10 mRNA
Fold Change
Control
PTH(1-34)
ABL
PTHrP(1-36)

4. Discussion

In this study we show that PTH (1-34), PTHrP (1-36), and ABL treatment of calvarial osteoblasts in vitro result in differing effects on the osteoblast transcriptome via RNA-Seq and additional qRT-PCR of several genes of interest. Previous research from our laboratory has shown PTH (1-34), PTHrP (1-36), and ABL exert time and dose-dependent differential responses in the osteoblast [36]. Many studies have examined PTH signaling in the osteoblast/osteocyte [7, 11, 14, 17, 27, 35, 36, 40], ours is the first to show that these peptides differentially modulate the osteoblast transcriptome in primary osteoblasts.

RNA-Sequencing data revealed PTH (1-34) regulated the most genes (367), followed by ABL (179 genes) and then by PTHrP (1-36) (116 genes), with PTH (1-34) generally having the greatest effects. Gene ontology analyses show biological processes are similar between the three peptides but have some pathway-specific differences. All 3 peptides regulated genes involved in ossification, cAMP signaling and epithelial cell proliferation, while PTH (1-34) and PTHrP (1-36), but not ABL, regulated genes of branching morphogenesis by GO. The latter may reflect the role of PTHrP in mammary gland development [41]. PTH (1-34) and ABL show an almost identical pattern otherwise, including 1) Wnt signaling, 2) nucleotide mediated signaling, 3) hormone transport and secretion, 4) endocrine processes, and 5) tissue development. PTHrP (1-36) regulates these pathways differently when compared with either of these peptides. Notably, PTH (1-34) and ABL similarly regulated genes of “bone mineralization”, “biomineral tissue development” and “actin filament bundle organization”, while PTHrP (1-36) did not regulate these pathways significantly. These similarities in pathway expression among

PTH (1-34) and ABL may explain why they have similar effects in vivo and why PTHrP (1-36), despite being an analog of ABL, did not have the same anabolic effects on bone mineral density [42].

Based on a close examination of the RNA-Sequencing data we selected a handful of genes that were significantly regulated by these peptides with either similar or differential expression patterns for confirmation via qRT-PCR. Additional mouse osteoblast samples were harvested for subsequent RNA isolation and additional analyses. From these data we were able to confirm several notable expression patterns elicited by these peptides in both the RNA-sequencing data and qPCR.

The first pattern of note which we found in both the qPCR and RNA-Sequencing data is that *Vdr*, *Cited1*, *Pde10a*, *Wnt11*, and *Sfrp4* followed the reported pattern of expression profiling of *Rankl* in response to these peptides: PTHrP (1-36) and ABL result in a moderate increase in gene expression compared with control with PTHrP (1-36) being, in most cases, significantly lower than ABL, and PTH (1-34) producing the greatest increase in expression of these genes compared with control (Fig 5).

VDR is an important factor in serum calcium homeostasis and with 1,25(OH)2 vitamin D3, is known to bind regulatory elements in the PTH gene promoter to block PTH transcription [43, 44]. A previous report showed that daily administration of PTH (1-34) for 48 h decreased renal *Vdr* mRNA expression by 15% in wild-type mice and determined that intermittent PTH (1-34) is a potent down-regulator of *Vdr* mRNA in vivo [45]. However, our data show that *Vdr* mRNA is increased by PTH (1-34) and this may be explained by the periodicity of treatment and cell type. In fact, one group showed that the PTH1R was present in mandibular/alveolar mouse bone at the earliest stages examined in

embryogenesis while the VDR only appeared later with maximal expression at E18 implying it may be induced by PTH or PTHrP action [46]. In a prehypertrophic chondrocyte cell line, PTHrP was shown to substantially increase *Vdr* expression and the authors suggested there was a functional paracrine feedback loop modulating chondrocyte differentiation [47]. In our case, the highest regulation by PTH (1-34) in osteoblastic cells intimates that this hormone may control 1,25(OH)2 vitamin D3 action on these cells.

The second gene showing the same pattern of regulation as *Rankl*, *Cited1*, has also been reported to be up-regulated significantly by PTH (1-34); Wt9 osteoblastic cells showed maximal upregulation of *Cited1* after 4 h of PTH treatment which was blocked by PKA inhibition [40]. They also observed that in calvarial osteoblasts derived from *Cited1* KO mice treated intermittently with a cAMP-selective analog of PTH, [G1,R19]hPTH (1-28), there were greater increases in mineralization, which identifies CITED1 as a negative regulator of osteoblast differentiation.

The general function of phosphodiesterases is to hydrolyze cyclic AMP and cyclic GMP second messenger molecules, thus regulating them as second messengers [48]. PDE10A has the highest affinity for cAMP and most of our knowledge on it comes from studies in the brain [49]. However, a recent study examined *PDE10A* expression in bone marrow-derived mesenchymal stromal cells isolated from a patient cohort undergoing hip replacement therapy [48]. They report that *PDE10A* is upregulated in response to mechanotransduction and that its upregulation impairs osteogenic signals and that an increase in cAMP was the key driver in the observed results. Our data show that *Pde10a* mRNA is upregulated significantly by all three peptides but with PTH (1-34) showing by far the largest increase in its expression. It is most likely that this is feedback regulation

to control cAMP concentrations and the highest induction by PTH (1-34) reflects the highest cAMP produced by this peptide in these cells.

SFRP4 has been shown to have deleterious effects on osteoblasts/osteocytes. SFRPs are well known antagonists of Wnt family signaling by directly binding the Wnts as decoy receptors or by forming nonfunctional Wnt complexes via Frizzled (Fz) proteins [50]. Canonical Wnt signaling typically promotes bone formation so any complex that removes or inhibits its function is likely to negatively affect osteoanabolic processes as shown in a study which utilized transgenic mice overexpressing SFRP4 and found that they exhibited comparatively lower bone mass [51]. The study concluded that this deleterious effect could be mostly attributed to a substantial suppression in bone proliferation/formation. Our data show that *Sfrp4* also has the highest upregulation in response to PTH (1-34) when compared to ABL and PTHrP (1-36) and may also be a feedback control mechanism in response to cAMP levels.

The effects of PTH (1-34) and its analogs on the osteoblast transcriptome illuminate the exquisite nature of bone modeling and remodeling. While several hundred genes are regulated by each peptide, we determined that pathway analysis would provide a more systematic way of analyzing the regulatory trends. Perhaps choosing an earlier time point would yield different results, particularly if performed to capture immediate early genes. Nonetheless, *Rankl*, *Vdr*, *Cited1*, *Pde10a*, *Sfrp4*, and *Wnt11*, which were differentially regulated in a similar pattern by the three peptides suggest that these are affected by the initial differences in cAMP/PKA signaling and may also involve the SIK/CRTC/bZIP pathway, which regulates *Rankl* transcription. Conversely, it is possible that the genes that were similarly regulated by all three peptides are governed by the

SIK/HDAC pathway as shown by the similar regulation of *Sost* and *Mmp13*, both of which are controlled through the SIK/HDAC arm. qRT-PCR analysis of these genes in calvarial osteoblasts treated with 8-bromo-cAMP, myr-PKI, si-SIKs, si-CRTCs, or si-HDACs would be able to confirm this hypothesis [36].

PTH and PTHrP are important factors for activating their common receptor PTHR1, typically thought to act through the cell surface with subsequent action via Gs and Gq/11 proteins, however recent findings suggest that internalized PTHR1, via Gαs and β-arrestin, can activate cAMP via endosomal signaling [52]. Depending on the ligand stabilizing PTHR1, the complex can assume different conformations and/or internalize itself in an early endosome. These different conformations then influence differences in downstream signaling. Ligands such as PTH may have sustained activation of PTHR1 due to their endosomal PTHR1/Gs/cAMP signaling favoring sustained action while PTHrP, with short and transient interactions via the cell membrane, may result in more transient effects [52].

The roles of the Wnt family may not be as clear cut based on our data and the data of previous research but many differences in expression within the Wnt family may be explained similarly by cell membrane vs endosomal signaling. Our pathway analyses and subsequent qPCR show that Wnt 4, Wnt 7b, and Wnt 11 all significantly increase their mRNA expression in response to all three peptide treatments compared to control but do not do so with the same pattern. Wnt 11 mimics the Rankl expression profile with PTH (1-34) having by far the maximal effect compared to ABL and PTHrP (1-36) while Wnt 4 / Wnt 7b expression was highest with PTHrP (1-36) and PTH (1-34) having a lesser effect. This may suggest that some Wnts (e.g., Wnt4) are regulated by signaling at the plasma

membrane by PTHrP while Wnt11 is regulated more highly by PTH via endosomal signaling. It is possible that the differences in ligand effects on the PTHR1 that occurs with these three peptides result in differential Wnt family expression profiles; PTHrP (1-36) causes greater signaling at the plasma membrane compared to PTH (1-34), while the latter results in greater endosomal signaling and therefore differential downstream effects.

The findings in this study highlight the complexity of the genetic and functional events that are triggered by PTH(1-34) and its analogs. Although we discovered many genes that seemingly fit into known paradigms there were many genes that should be further evaluated to understand the importance of PTHR1 and how it affects downstream signaling. A closer examination of some of these genes might reveal intricacies in the interactions of PTHR1 and PTH-derived treatments just as further delineation of which events are attributable to signaling mechanisms triggered by PTH(1-34), PTHrP (1-36), and ABL would allow for further refining of future treatments for osteoporosis.

5. Acknowledgements

This work was supported by the National Institutes of Health (grant numbers DK047420, DK047420-23S1, DK126539).

References

1) Johnell O, Kanis JA. An estimate of the worldwide prevalence and disability associated with osteoporotic fractures. Osteoporos Int 2006;17(12):1726-33
2) Raggatt LJ, Partridge NC. Cellular and molecular mechanisms of bone remodeling J Biol Chem. 2010;285(33): 25103–25108
3) Harvey N, Dennison E, Cooper C. Osteoporosis: impact on health and economics. Nat. Rev. Rheumatol. 2010;6:99–105
4) Canalis E, Giustina A, Bilezikian JP. Mechanisms of anabolic therapies for osteoporosis. N Engl J Med 2007;357:905-16
5) Pazianas M, Abrahamsen B. Osteoporosis treatment: bisphosphonates reign to continue for a few more years, at least? Ann N Y Acad Sci 2016;1376(1):5-13
6) Strewler GJ, Rosenblatt M. Mineral metabolism. In: Endocrinology and Metabolism. New York: McGraw-Hill, Inc; 1995
7) Jilka RL, Weinstein RS, Bellido T et al. Increased bone formation by prevention of osteoblast apoptosis with parathyroid hormone. J Clin Invest 1999;104(4):439-446
8) Nishida S, Yamaguchi A, Tanizawa T. Increased bone formation by intermittent parathyroid hormone administration is due to the stimulation of proliferation and differentiation of osteoprogenitor cells in bone marrow. Bone 1994;15(6):717-723
9) Matic I, Matthews BG, Wang X et al. Quiescent bone lining cells are a major source of osteoblasts during adulthood. Stem Cells 2016;43(12):2930-2942
10) Poole KE, van Bezooijen RL, Loveridge N et al. Sclerostin is a delayed secreted product of osteocytes that inhibits bone formation. FASEB J 2005;19(13):1842-1844
11) Bellido T, Ali AA, Gubrij I et al. Chronic elevation of parathyroid hormone in mice reduces expression of sclerostin by osteocytes: a novel mechanism for hormonal control of osteoblastogenesis. Endocrinology 2005;146(11):4577-4583
12) Siddiqui JA, Partridge NC. CCL2/Monocyte chemoattractant protein 1 and parathyroid hormone action on bone. Front Endocrinol (Lausanne) 2017 Mar 29;8:49.
13) Simonet WS, Lacey DL, Dunstan CR et al. Osteoprotegerin: a novel secreted protein involved in the regulation of bone density. Cell. 1997;89(2):309-319
14) Huang JC, Sakata T, Pfleger LL et al. PTH differentially regulates expression of RANKL and OPG. J Bone Miner Res 2004;19(2):235-244
15) Nakatani T, Chen T, Partridge NC. MMP-13 is one of the critical mediators of the effect of HDAC4 deletion on the skeleton. Bone. 2016 Sep; 90: 142–151.
16) Baron R, Hesse E. Update on bone anabolics in osteoporosis treatment: rationale, current status, and perspectives. J. Clin. Endocrinol. Metab. 2012;97(2):311–325
17) Fu Q, Jilka RL, Manolagas SC et al. Parathyroid hormone stimulates receptor activator of NFkappa B ligand and inhibits osteoprotegerin expression via protein kinase A activation of cAMP-response element-binding protein. J. Biol. Chem. 2002;277(50):48868–48875
18) Nakashima T, Hayashi M, Fukunaga T et al. Evidence for osteocyte regulation of bone homeostasis through RANKL expression. Nat. Med. 2011;17(10):1231–1234
19) Xiong J, O'Brien CA. Osteocyte RANKL: new insights into the control of bone remodeling. J. Bone Miner. Res. 2012;27(3):499–505

20) Sleeman A, Clements JN. Abaloparatide: A new pharmacological option for osteoporosis. Am J Health Syst Pharm. 2019;76(3):130-135
21) Neer RM, Arnaud CD, Zanchetta JR, et al. Effect of parathyroid hormone (1–34) on fractures and bone mineral density in postmenopausal women with osteoporosis. N. Engl. J. Med. 2001;344, 1434 –1441
22) Leder BZ. Parathyroid hormone and parathyroid hormone-related protein analogs in osteoporosis therapy. Curr Osteoporos Rep. 2017;15(2):110–119
23) Miller PD, Hattersley G, Riis BJ, et al. Effect of abaloparatide vs placebo on new vertebral fractures in postmenopausal women with osteoporosis: a randomized clinical trial. JAMA 2016;316, 722–733
24) Brent MB. Abaloparatide: A review of preclinical and clinical studies. Eur J Pharmacol 2021 Oct 15;909:174409.
25) Le Henaff C, Partridge NC. PTHR in Bone. In “GPCRs as Therapeutic Targets”, November 2022, Edited by Annette Gilchrist, Wiley
26) Hattersley G, Dean T, Corbin BA, et al. Binding selectivity of abaloparatide for PTH-type-1-receptor conformations and effects on downstream signaling. Endocrinology 2016;157, 141–149
27) Cheloha RW, Gellman SH, Vilardaga JP, et al. PTH receptor-1 signalling-mechanistic insights and therapeutic prospects. Nat. Rev. Endocrinol. 2015;11, 712–724
28) Gardella TJ, Vilardaga JP. International union of basic and clinical pharmacology. XCIII. The parathyroid hormone receptors--family B G protein-coupled receptors. Pharmacol Rev 2015;67(2):310-37.
29) Yang D, Singh R, Divieti P, et al. Contributions of parathyroid hormone (PTH)/PTH-related peptide receptor signaling pathways to the anabolic effect of PTH on bone. Bone 2007;40, 1453–1461
30) Fu Q, Manolagas SC, O’Brien CA. Parathyroid hormone controls receptor activator of NF-kB ligand gene expression via a distant transcriptional enhancer. Mol. Cell. Biol. 2006;26,6453– 6468
31) Kim S, Yamazaki M, Shevde NK, Pike JW. Transcriptional control of receptor activator of nuclear factor-kB ligand by the protein kinase A activator forskolin and the transmembrane glycoprotein 130-activating cytokine, oncostatin M, is exerted through multiple distal enhancers. Mol. Endocrinol. 2007;21,197–214
32) Nakashima T, Hayashi M, Fukunaga T, et al. Evidence for osteocyte regulation of bone homeostasis through RANKL expression. Nat. Med. 2011;17,1231–1234
33) Xiong J, Onal M, Jilka RL, et al. Matrix-embedded cells control osteoclast formation. Nat. Med. 2011;17,1235–1241
34) Xiong J, O’Brien CA. Osteocyte RANKL: new insights into the control of bone remodeling. J. Bone Miner. Res. 2012;27, 499 –505
35) Saini V, Marengi DA, Barry KJ, et al. Parathyroid hormone (PTH)/PTH-related peptide type 1 receptor (PPR) signaling in osteocytes regulates anabolic and catabolic skeletal responses to PTH. J. Biol. Chem. 2013;288,20122–20134
36) Ricarte FR, Le Henaff C, Kolupaeva VG, et al. Parathyroid hormone(1−34) and its analogs differentially modulate osteoblastic Rankl expression via PKA/SIK2/SIK3 and PP1/PP2A−CRTC3 signaling J. Biol. Chem. 2018, 293:20200-20213.

37) Patro R, Duggal G, Love MI, Irizarry RA. Kingsford C. Salmon provides fast and bias aware quantification of transcript expression. Nat Methods. 2017;14(4):417-419
38) Love MI, Huber W, Anders S. Moderated estimation of fold change and dispersion for RNA-seq data with DESeq2. Genome Biol 2015;15,550
39) Huang D, Sherman B, Lempicki R. Systematic and integrative analysis of large gene lists using DAVID bioinformatics resources. Nat Protoc 2009;4,44–57
40) Yang D, Guo J, Divieti P et al. CBP/p300-Interacting Protein CITED1 modulates parathyroid hormone regulation of osteoblastic differentiation. Endocrinology. 2008 Apr; 149(4): 1728–1735.
41) Hiremath M, and Wysolmerski J. Parathyroid hormone-related protein specifies the mammary mesenchyme and regulates embryonic mammary development. J Mammary Gland Biol Neoplasia. 2013 Jun; 18(2): 171–177
42) Le Henaff C, Ricarte FR, Finnie B et al. Abaloparatide at the same dose has the same effects on bone as PTH (1-34) in mice. J Bone Miner Res 2020 Apr;35(4):714-724.
43) Pike JW, Meyer MB, Watanuki M et al. Perspectives on mechanisms of gene regulation by 1,25-Dihydroxyvitamin D3 and its receptor. J Steroid Biochem Mol Biol. 2007 Mar; 103(3-5): 389–395.
44) Pike JW, Meyer MB. The vitamin D receptor: new paradigms for the regulation of gene expression by 1,25-Dihydroxyvitamin D3. Endocrinol Metab Clin North Am. 2010 Jun; 39(2): 255–269.
45) Healy KD, Vanhooke JL, Prahl JM et al. Parathyroid hormone decreases renal vitamin D receptor expression in vivo. Proc Natl Acad Sci U S A. 2005 Mar 29; 102(13): 4724–4728.
46) Bobek J, Oralova V, Lesot H et al. Onset of calciotropic receptors during the initiation of mandibular/alveolar bone formation. Ann Anat 2020;227:151427
47) Bach FC, Rutten K, Hendriks K et al. The paracrine feedback loop between vitamin D_3 (1,25$(OH)_2D_3$) and PTHrP in prehypertrophic chondrocytes. J Cell Physiol. 2014;229(12):1999-2014.
48) Deubert SM, Ege C, Krug M et al. Phosphodiesterase 10A Is a mediator of osteogenic differentiation and mechanotransduction in bone marrow-derived mesenchymal stromal cells. Stem Cells Int. 2020; 2020: 7865484.
49) Wilson LS, Brandon NJ. Emerging biology of PDE10A. Current Pharmaceutical Design. 2015;21(3):378–388.
50) Kawano Y, Kypta R . Secreted antagonists of the Wnt signalling pathway. J Cell Sci 2003;116:2627–2634
51) Nakanishi R, Akiyama H, Kimura H et al. Osteoblast-targeted expression of Sfrp4 in mice results in low bone mass. J Bone Miner Res. 2008 Feb;23(2):271-7
52) Vilardaga JP, Gardella TJ, Wehbi VL et al. Non-canonical signaling of the PTH receptor. Trends Pharmacol Sci. 2012 Aug; 33(8): 423–431.

APPENDIX A

Mouse Primers (5'—3')

	Forward	Reverse
Cited1	GAGGCCTGCACTTGATGTC	TGGAGTAGGCCAGAGAGTTCA
Vdr	TATTCTCCAAGGCCCACACT	GATCCATCGTGGAAAAGCTG
Pde10a	CGACCTCGCCCTATACTTTG	CATCATCAAGCCGATGACAC
Wnt11	TAGGGCCTTCGCTGACAT	GGCATACACGAAGGCTGACT
Sfrp4	TGGAGAGATCAACTCAGTAGAAGG	GGCTGGCTATCTGCTTCTTG
Crem	GTAGCTGGATCAGGCACTGG	CGGCTGATTGTGCTGCATAC
Epha3	GCGCCTTCACTTTGGGAATG	TCCAACTCCTTCGCGAACTC
Hdac4	GTGTGGATTTAGCCTGTTGGTT	CCCTGGCAGTCCAAAGATGT
Pp2r2a	GAGACAAAAGACCAGAAGGCTATA	ATTCTCCGTGGACTGGCTTCCA
Dvl3	CCCTCCTTAAGCACCATCAC	TGTCACTGTGGATGGAGAGG
Wnt4	CCCTCGCAGTTTTGTCCTCT	CATGGGAGCCACTTGGACAT
Wnt7b	GTCTTCGGGCAAGAACTCC	TCACAGCCACAATTGCTCA
Dkk1	CCAACGCGATCAAGAACCTG	GTACTTGTTCCCGCCCTCAT
Fzd5	TGTCGTTAAACTTTCCCAGCTC	TCCGACTCCAAGGACAGAAC
Tcf7	TGCTGGGATCTGGTGTACC	TGCCTGTGTTTTCAGGTTTCT
Kcnk10	CCCGGCTCTTTGATCCTCTC	AACAGGGTGATGCCCGTTAG
β-actin	TCCTCCTGAGCGCAAGTACTCT	CGGACTCATCGTACTCCTGCTT
Rankl	GCTCCGAGCTGGTGAAGAAA	CCCCAAAGTACGTCGCATCT
Rpl13	CTGCTCTCAAGGTTGTTCGGCT	CCTTCCGTTTCTCCTCCAGAGT